ECOLOGY LETTERS

Volume 20 Number 11 | November 2017

Cover Caption: Dead trunk of a *Fagus sylvatica* tree photographed near Peaston (Scotland) after a drought episode.
Photo Credit: Dr. Hervé Cochard (INRA, Clermont-Ferrand, France)
From: Syvain Delzon, p.1437

WILEY

cnrs advancing the frontiers

ISSN 1461-023X www.ecologyletters.com

Ecology Letters, (2017) doi: 10.1111/ele.12851

LETTER

Plant resistance to drought depends on timely stomatal closure

Nicolas Martin-StPaul,[1] Sylvain Delzon[2]* and Hervé Cochard[3]

[1]*URFM, INRA, 84000, Avignon, France*
[2]*BIOGECO, INRA, Univ. Bordeaux, 33615, Pessac, France*
[3]*Université Clermont-Auvergne, INRA, PIAF, 63000, Clermont-Ferrand, France*

**Correspondence: E-mail: sylvain.delzon@u-bordeaux.fr*

Abstract

Stomata play a significant role in the Earth's water and carbon cycles, by regulating gaseous exchanges between the plant and the atmosphere. Under drought conditions, stomatal control of transpiration has long been thought to be closely coordinated with the decrease in hydraulic capacity (hydraulic failure due to xylem embolism). We tested this hypothesis by coupling a meta-analysis of functional traits related to the stomatal response to drought and embolism resistance with simulations from a soil–plant hydraulic model. We report here a previously unreported phenomenon: the existence of an absolute limit by which stomata closure must occur to avoid rapid death in drought conditions. The water potential causing stomatal closure and the xylem pressure at the onset of embolism formation were equal for only a small number of species, and the difference between these two traits (i.e. safety margins) increased continuously with increasing embolism resistance. Our findings demonstrate the need to revise current views about the functional coordination between stomata and hydraulic traits and provide a mechanistic framework for modeling plant mortality under drought conditions.

Keywords

Dieback, drought, stomata, tree mortality, xylem embolism.

Ecology Letters (2017)

INTRODUCTION

Recent drought episodes have been identified as the triggers for widespread plant mortality events around the world (Allen *et al*. 2010; Carnicer *et al*. 2011; Park Williams *et al*. 2012). They have had huge consequences for the productivity of the land (Ciais *et al*. 2005) and have undoubtedly affected a panel of ecosystem services (Anderegg *et al*. 2012). Identifying the mechanisms and traits underlying drought resistance will be essential if we have to understand and predict the impact of widespread droughts over many land areas. Experimental studies have provided empirical evidence that failure of the water transport system is tightly linked to tree desiccation and mortality in drought conditions. Support for this hypothesis was recently provided by a study reporting that hydraulic traits explain cross-species patterns of drought-induced mortality at the global scale (Anderegg *et al*. 2016). Two types of traits are thought to be involved in plant hydraulic failure under drought conditions: hydraulic traits ensuring the integrity of the hydraulic system under water deficit (Choat *et al*. 2012), and stomatal traits controlling gas exchange at the leaf surface (Klein 2014). However, efforts to model tree mortality in response to drought are hindered by a lack of understanding of how and why these traits covary at the global scale, and interact to define physiological dysfunctions under drought stress (McDowell *et al*. 2013). In this study, we analysed the overall connections between these two types of traits for the full range of drought resistance, using a soil–plant hydraulic model, and we provide a new formal framework for predicting plant mortality under drought.

The stomata have two key functions: controlling transpiration, which supplies nutrients and regulates leaf temperature, and controlling the entry of CO_2 into the leaf. Stomatal closure in response to water deficit is the primary limitation to photosynthesis (Flexas & Medrano 2002), and constitutes a key cost in terms of plant growth and temperature regulation under drought conditions. However, stomatal closure also limits excessive decreases in water potential (quantified as a negative pressure, ψ) in the plant, thereby ensuring that water demand from the leaves does not exceed the supply capacity of the hydraulic system, which would lead to embolism of the vascular system and complete desiccation of the plant. These key, but opposing roles of stomata in regulating CO_2 influx and H_2O loss pose a dilemma that has occupied scientists for centuries (Bessey 1898; Darwin 1898) and has led to the view that plant stomata probably operate at the edge of the supply capacity of the plant's hydraulic system, to balance different costs, such as productivity and leaf temperature regulation during drought (Tyree & Sperry 1988; Cruiziat *et al*. 2002; Sperry 2004).

Conversely, maintenance of the supply capacity of the hydraulic system depends on the ability of a species to resist embolism at the highly negative pressure caused by soil water deficit. Embolism resistance is usually quantified as the value of ψ causing 50% embolism (Ψ_{50}), and the rate of embolism spread per unit drop in water potential (*slope*). From these two traits, the Ψ at the onset of embolism formation can be calculated (Ψ_{12}, Text S1), providing a more conservative estimate of the functional limit to the hydraulic system. Embolism resistance varies considerably between species and with the dryness of species habitat (Maherali *et al*. 2004; Choat *et al*. 2012; Lens *et al*. 2016; Larter *et al*. 2017). A recent study suggested that hydraulic systems highly resistant to embolism evolved in response to the selective pressure associated with increasing drought levels during a paleoclimatic crisis (Pittermann *et al*. 2012; Larter *et al*. 2017). Some contemporary plants have extremely drought-resistant vascular

systems, with Ψ_{50} values reaching −19 MPa (Larter *et al.* 2015).

These findings have led to the suggestion that an efficient match between the capacity of the hydraulic system to sustain water deficit (i.e. embolism resistance) and the regulation of demand by the stomata is a prerequisite for the maximisation of gas exchange without desiccation (Tyree & Sperry 1988; Jones & Sutherland 1991; Sperry *et al.* 1998; Sperry 2004). This notion naturally leads to the hypothesis that stomatal behaviour and embolism resistance have followed a similar evolutionary trajectory under drought constraints, and that plants have increased their intrinsic embolism resistance to allow stomata to close later during drought, thereby maximising plant productivity (Cruiziat *et al.* 2002; Klein 2014; Skelton *et al.* 2015; Anderegg *et al.* 2016). The coordination of stomatal and hydraulic traits and their role in shaping drought resistance have yet to be addressed on a global scale. Such studies would help to clarify the interplay between mechanisms and plant traits in defining the physiological dysfunctions occurring under drought stress, which remains one of the principal challenges faced in the modelling of tree mortality in response to drought.

In this study, we gathered data for different stomatal regulation traits and embolism resistance traits for more than 100 species from different biomes, to explore their covariation empirically over the full range of drought resistance. We then used a soil–plant water transport model to elucidate how different associations between Ψ_{close} and Ψ_{50} determine the time until hydraulic failure during drought. We validated model predictions, using empirical data for time to shoot death collected in drought mortality experiments (Brodribb & Cochard 2009; Barigah *et al.* 2013; Urli *et al.* 2013; Li *et al.* 2015), to provide a conceptual framework for predicting plant mortality under drought conditions.

MATERIALS AND METHODS

Data meta-analysis

Various measurement artefacts are known to have tainted embolism measurements in recent decades (Cochard *et al.* 2013, 2015), and recent direct observations of the xylem content by X-ray tomography have confirmed the need for caution when selecting embolism data (Beikircher *et al.* 2010; Choat *et al.* 2014, 2016; Cochard *et al.* 2015; Torres-Ruiz *et al.* 2015). We chose to use a conservative dataset for this study. We therefore calculated ψ_{12}, ψ_{50} and *slope* from S-shaped vulnerability curves obtained and published by our group over the last 20 years (details in Text S1, Table S1). All stem vulnerability curves were fitted with a sigmoidal function (Vander Willigen & Pammenter 1998):

$$PLC\frac{1}{1+e^{\left(\frac{slope}{25}\left(\Psi_{plant}-\psi_{50}\right)\right)}} \quad (1)$$

where PLC is the percent loss of plant hydraulic conductance due to embolism, ψ_{plant} is the xylem water potential, ψ_{50} is the water potential causing a 50% loss of plant hydraulic conductivity and *slope* (%/MPa) is a shape parameter describing the rate of embolism spread per unit water potential drop at the ψ_{50}. The ψ_{12} can be calculated from ψ_{50} and *Slope* ($\psi_{12} = \psi_{50} + 50/Slope$). For all the species for which data for stem embolism resistance traits are available, we collected data for different traits indicating the level of plant water deficit (Ψ) causing the highest degree of stomatal closure (hereafter referred to as Ψ_{close}). We first used concomitant measurements of gas exchange and leaf water potential, from which the Ψ value at 90% stomatal closure was calculated as previously described (Klein 2014; Mencuccini *et al.* 2015; Bartlett *et al.* 2016). Stomatal opening increases with guard cell turgor pressure (Franks *et al.* 1998; Buckley 2005), and it has been shown that stomatal closure in woody species is largely explained by losses of leaf turgor (Brodribb *et al.* 2003; Rodriguez-Dominguez *et al.* 2016). We therefore also used leaf water potential at turgor loss (Ψ_{tlp}) as a surrogate for Ψ_{close}, when Ψ_{gs90} was not available (see details on data acquisition in Text S2). Embolism resistance and Ψ_{close} data were collected from plants at all stages of development, but a comparison between small (mostly seedlings) and large plants (mostly adults) indicated that data for plants of different statures were comparable, at least in the context of a meta-analysis (Text S3, Figure S1).

We studied the statistical associations between the two different types of traits by fitting three different models (linear, sigmoidal and segmented models, Text S4). The segmented model provided the best fit to the data based on AIC (Table S2) and was retained for subsequent analyses. First, the fitted segmented regression between Ψ_{close} (or its component Ψ_{tlp} or Ψ_{gs90}) and embolism resistance (Ψ_{50} or Ψ_{12}) was used to identify (1) the break points in the *x* axis (i.e. the embolism resistance value at which there is a change in the covariation between Ψ_{close} and embolism resistance) and (2) the *y* axis intercept for this break point (i.e. the global limit for Ψ_{close}). Second, we calculated the correlation coefficient and the linear regression between Ψ_{close} and embolism resistance for the data on either side of the break point. In addition to the results reported in the main manuscript, we provide separate analyses for gymnosperms and angiosperms and for each trait (ψ_{50}, ψ_{12}, ψ_{gs90} and ψ_{tlp}) in Table S2, Table S3, Figure S3 and Figure S4. All the parameters used in this study are provided in a supplementary Excel file '*Database.xlsx*'.

SUREAU MODEL: DESCRIPTION, SIMULATION AND VALIDATION

SurEau is a simplified discrete-time soil–plant hydraulic model used to simulate the time to hydraulic failure for the range of embolism resistance values reported in our database, under different hypotheses concerning the stomatal regulation of transpiration. SurEau assumes that plant death in severe drought conditions is due to desiccation, which is modelled through the process of cavitation. The system has been simplified to consider only two resistances (rhizosphere and plant), making it easy to apply, with only one stem vulnerability curve and no need for assumptions concerning hydraulic segmentation, a phenomenon dependent on mechanisms that remain a matter of debate (Bouche *et al.* 2015, 2016a,b; Cuneo *et al.* 2016; Scoffoni *et al.* 2017; Skelton *et al.* 2017).

Description of the SurEau model

SurEau calculates soil and plant water status and assesses embolism by assuming that liquid water flow through the soil–plant system is exactly compensated by gaseous water losses at the surface of the foliage of the plant (i.e. steady-state conditions). Our general approach is inspired by many previous studies (Whitehead & Jarvis 1981; Tyree & Sperry 1988; Sperry *et al*. 1998; Tuzet *et al*. 2003) and has already been shown to apply to large time steps (>1 day) and small plants (Rambal 1993; Tuzet *et al*. 2003). The model also assumes that leaf and air temperatures are equal, to avoid the need to describe leaf energy balance. We can therefore write:

$$E = g_l \times \mathrm{VPD} = k_{sl} \times \left(\Psi_{\mathrm{soil}} - \Psi_{\mathrm{plant}}\right) \quad (2)$$

where E is transpiration, g_l is leaf conductance for vapour water, VPD is the vapour pressure deficit between air and leaf, ψ_{soil} is the soil water potential, ψ_{plant} is plant water potential and K_{sl} is the plant leaf area-specific hydraulic conductance over the soil to leaf pathway. g_l includes the stomatal, cuticular and boundary layer conductances of the leaf. The control of E through stomata is treated through several assumptions described below. k_{sl} was calculated as the result of two conductances in series:

$$k_{sl} = \frac{1}{\frac{1}{k_{\mathrm{soil}}} + \frac{1}{k_{\mathrm{plant}}}} \quad (3)$$

where K_{soil} is the hydraulic conductance of the soil-to-root surface pathway and K_{plant} is the hydraulic conductance of the whole plant (i.e. from the roots to the leaves). K_{plant} was allowed to vary only to account for the loss of hydraulic conductivity caused by xylem embolism (Tyree & Ewers 1991):

$$k_{\mathrm{plant}} = k_{\mathrm{Pini}}(1 - \mathrm{PLC}) \quad (4)$$

where K_{Pini} is the initial (i.e. pre-drought) plant hydraulic conductance and PLC is the percent loss of plant hydraulic conductance due to xylem embolism. PLC is calculated at each time step from the sigmoidal function for the vulnerability curve (VC) for embolism (see eqn 1).

We considered two different plant water reservoirs (Tyree & Yang 1990). The first, the apoplastic reservoir, consists of the inelastic xylem cells that release their water to the transpiration stream following embolism. This reservoir accounts for a large proportion of the water in stems [> 80%, (Tyree & Yang 1990)] and is thought to be an important parameter for plant survival during drought episodes (Tyree & Yang 1990; Hölttä *et al*. 2009). The water freed by air filling feeds the water stream of the system, thereby tempering the decrease in water potential (Hölttä *et al*. 2009). As suggested by Hölttä *et al*. (2009), we considered any change in PLC to be followed by a proportional change in the volume of water released back to the system:

$$W_{xv} = V_X \times \mathrm{PLC} \quad (5)$$

where W_{xv} is the amount of water released to the system and V_X is the total water-filled xylem volume of the plant (m^3) and PLC is defined in eqn 1. V_X was calculated as:

$$V_X = E_{md} \times LA \times G \times \alpha_f \quad (6)$$

where E_{md} is the maximum diurnal transpiration (calculated from the maximal transpiration rate and assuming 10 h of transpiration per day), LA is leaf area, α_{f} is the apoplastic fraction of the plant and G is the ratio of the total amount of water in the tree to maximum daily transpiration. The second reservoir considered was that formed by the elastic water release due to symplasm dehydration (i.e. the water released by the symplastic tissue $1-\alpha_{\mathrm{f}}$). The dynamics of this reservoir depend on osmotic potential and the elasticity of the cell walls, which may either stretch or contract to allow water to flow in or out with changing ψ. This reservoir therefore constitutes an elastic form of storage, in which variation occurs at relatively high water potential (typically >-3 MPa, Tyree & Yang 1990) and it can be described by pressure volume curves combined with the same formula as for cavitation (eqn 5). Symplastic water volume was thus calculated as in eqn 6 but with the symplastic fraction ($1-\alpha_{\mathrm{f}}$) of the plant. The release of water from the symplastic reservoir (W_{sv}) was computed as in eqn 5, with PLC replaced by the relative water content of the symplasm (R_{s}). R_{s} was calculated from ψ_{leaf} by inverting the classical pressure–volume curve equations (Appendix S3).

Variations of soil and rhizophere conductance (K_{soil}), and mean soil water potential in the root zone are calculated with van Genuchten–Mualem equations (Mualem 1976; van Genuchten 1980), from the unsaturated hydraulic conductivity of the soil (k_{soil}), scaled to the rhizophere according to the Gardner–Cowan formulation (Gardner 1964; Cowan 1965). Rhizophere conductance can be expressed as:

$$K_{\mathrm{soil}} = B \times k_{\mathrm{soil}}(\Theta) \quad (7)$$

where k_{soil} is the unsaturated hydraulic conductivity of the soil at a given water content (Θ) or water potential (see below) and B is the root density conductance factor accounting for the length and geometry of the root system. B is based on the implicit assumption of a uniform root distribution in a soil layer, according to the Gardner–Cowan formulation (Gardner 1964; Cowan 1965). B is also called the 'single root' approach (Tardieu *et al*. 1992) as it is equivalent to assuming that plant water uptake occurs from a unique cylindrical root that has access to a surrounding cylinder of soil:

$$B = \frac{2\pi L_a}{\ln\left(\frac{b}{r}\right)} \text{ with } b = \frac{1}{\sqrt{\pi L_v}} \quad (8)$$

where L_a is the root length per unit area, r the mean root radius, and b is half the mean distance between neighbouring roots. b can be evaluated from L_{v}, the root length per unit soil volume. k_{soil} decreases with decreasing ψ_{soil} because of the displacement of water from pores by air, as the capillary forces linking water to soil particles fail with increasing tension, thus creating dry non-conductive zones in the rhizosphere. Van Genuchten's parametric formulation (van Genuchten 1980) for the water retention curve was used together with the equation of Mualem (1976) to calculate ψ_{soil} and the unsaturated hydraulic conductivity of the soil as a function of soil relative extractable water content (Θ). ψ_{soil} can be calculated as follows:

$$\Psi_{soil} = \frac{\left(\left(\frac{1}{\Theta}\right)^{\frac{1}{m}} - 1\right)^{\frac{1}{n}}}{\alpha}; m = 1 - \frac{1}{n} \quad (9)$$

where m, n and α are empirical parameters describing the typical sigmoidal shape of the function. Mualem (1976) provided a formula for changes in hydraulic conductivity with soil water content $k_{soil}(\Theta)$:

$$k_{soil} = k_{sat}\Theta^{l} \times \left[1 - \left(1 - \Theta^{\frac{1}{m}}\right)^{m}\right]^{2} \quad (10)$$

where k_{sat} is the saturated hydraulic conductivity, l is a parameter describing the pore structure of the material (usually set to 0.5), and m is again set as in eqn 9. The relative extractable water content (Θ) is expressed as follows:

$$\Theta = \frac{\theta - \theta_r}{\theta_s - \theta_r} \quad (11)$$

where θ is the relative water content (soil water content per unit soil volume), θ_s is the relative soil water content at saturation (or field capacity) and θ_r is the relative soil water content at wilting point. θ_s and θ_r are parameters measured in the laboratory or derived from soil surveys with pedotransfer functions. By contrast, θ is variable, changing dynamically with changes in absolute soil water reserve in the rooting zone (WR). The parameters and the sensitivity analysis are provided in Appendix S4.

Dynamic simulations

Under well-watered conditions, transpiration (E) is forced at a constant value, assuming a constant high vapour pressure deficit. At each time step, the soil water reserve (WR) is calculated and then used to calculate all the other variables. WR is then calculated as the result of water balance:

$$WR_{t+1} = WR_t - E + W_{xv} + W_{sv} \quad (12)$$

where E is the cumulative transpiration over the time step, W_{xv} is water release due to cavitation and W_{sv} is water release due to symplasm dehydration (eqns 5 and 6 and the corresponding text). The time step was set to 0.1 days, but increasing this value to 0.5 or decreasing it had little influence on the general pattern of the results obtained. E was calculated as follows:

$$E = [E_{max} \times f(\psi_{plant})] \times LA \quad (13)$$

where E_{max} is the maximal transpiration rate, LA is plant leaf area and $f(\psi_{plant})$ is the stomatal regulation function, which was set according to various hypotheses, as described below. The calibrations for E_{max}, LA, and all the other parameters are provided in Appendix S4.

Testing of hypotheses concerning the relationship between ψ_{close} and ψ_{50}

We used the model described above to evaluate the role of ψ_{close} and ψ_{50} in determining survival time until hydraulic failure under drought conditions for the full range of embolism resistance reported in the database. Three different hypotheses regarding the transpiration-regulating function of stomata were tested to obtain insight into the ways in which interplay between stomatal closure and embolism resistance shape survival under drought conditions (Fig. 2a). For the baseline simulation, we assumed that stomata never close ($\psi_{close} = -\infty$), and thus do not regulate transpiration (E) at all during drought, whatever the soil and plant water potential. This simplistic assumption was used to assess the effect of stomatal closure developed in hypotheses 2 and 3, described below. The second hypothesis tested was the widely accepted idea that stomata must close as soon as an embolism forms (corresponding to a tight match between ψ_{close} and ψ_{12}). This hypothesis was modelled by assuming that the point at which leaf turgor is lost corresponds to the water potential causing incipient embolism (i.e. $\psi_{close} = \psi_{12}$) over the entire embolism resistance spectrum. E regulation was modelled assuming progressive stomatal closure with the loss of leaf turgor, with a quadratic solution for pressure–volume equations (Vitali *et al.* 2016; Appendix S3). Once turgor is lost, the stomata are fully closed and E is reduced to a residual component corresponding to cuticular losses and stomatal leakiness due to imperfect closure (Brodribb *et al.* 2014). Finally, in our third hypothesis, the stomata regulate E in a timely manner following the onset of drought, such that ψ_{close} covaries with ψ_{12} until $\psi_{close} = -3$ MPa, in accordance with the typical pattern reported for empirical data (see Results, Fig. 1c). Stomatal closure was simulated through turgor loss as in hypothesis 2. For each of these hypotheses, survival (taken as the number of days before 100% PLC is reached) was calculated for the full range of embolism resistance encountered in our database, (i.e. from $\psi_{50} = -1.5$ to $\psi_{50} = -19$ MPa, in 1 MPa steps). A detailed analysis of these simulations is provided in Appendix S2.

Model validation: survival during drought, based on drought mortality experiments

For validation of the simulated relationship between survival and P_{50}, we built an empirical relationship between the survival measured in drought mortality experiments and embolism resistance. We collected mortality data for 15 species, covering a wide range of embolism resistance (ψ_{50} from -1.5 to -11) from four different drought mortality experiments published in recent years (Brodribb & Cochard 2009; Barigah *et al.* 2013; Urli *et al.* 2013; Li *et al.* 2015). One study concerned gymnosperm species only (Brodribb & Cochard 2009) and three other studies were performed on angiosperm species only (Barigah *et al.* 2013; Urli *et al.* 2013; Li *et al.* 2015). All these experiments were conducted under semicontrolled conditions, on seedlings or saplings in pots, and the drought treatment consisted of a cessation of watering until death. All studies recorded mortality estimated visually as the percentage of leaf or shoot death at various time points in the experimental drought period. We calculated the average time taken to reach 50% shoot death (T_{50}) since the last watering in these studies, which we used as an indicator of survival during drought. Soil volume and climate were identical for all species in each experiment. However, the relative humidity of the air and soil volume differed between experiments (both these factors can strongly affect survival time during an episode of

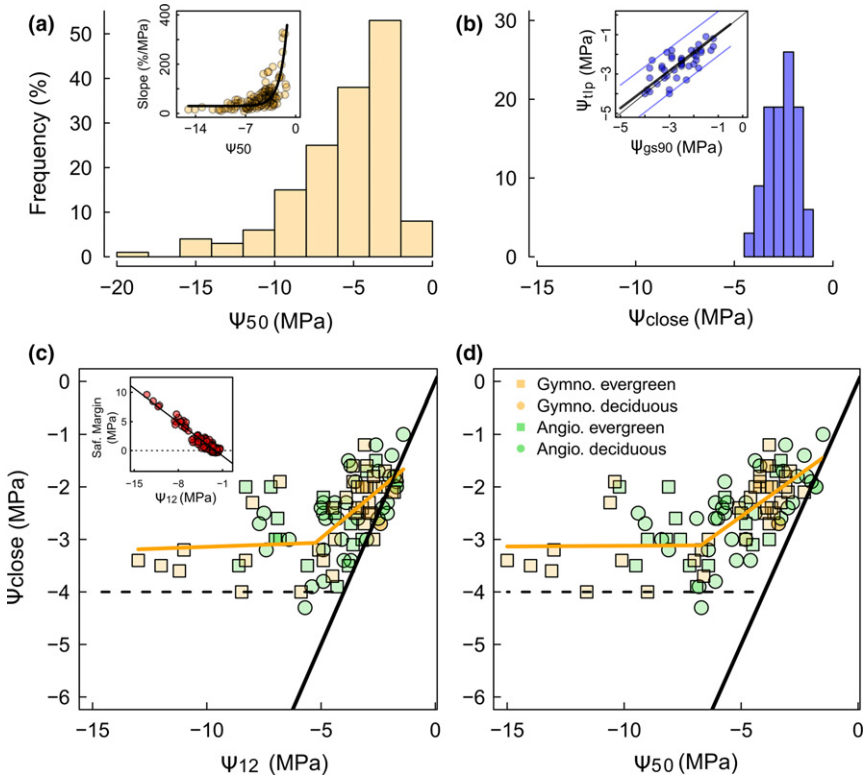

Figure 1 Range of variation of embolism resistance (Ψ_{50}) and stomatal response to drought (Ψ_{close}), and their covariation. (a) Distribution of embolism resistance (Ψ_{50}) among plants. The inset shows the relationship between the *slope* of the vulnerability curve (%/MPa, Text S1) and Ψ_{50}, making it possible to calculate Ψ_{12} (MPa). The best fit was obtained with $slope = 16 + e^{(\psi 50)} \times 1092$, the fitted parameters were significantly different from 0 ($P < 0.01$). (b) Distribution of the water potential causing stomatal closure (Ψ_{close}). The relationship between the two different traits for Ψ_{close} (the water potential causing 90% stomatal closure, Ψ_{gs90}) and the water potential causing leaf turgor loss (Ψ_{tlp}) is shown in the inset with the fitted line ($\psi_{tlp} = 0.97 \times \psi_{gs90}$, $P < 0.01$, $R^2 = 0.4$) and the 95% confidence interval. (c) The relationship between Ψ_{close} and Ψ_{12}, (d) Relationship between Ψ_{close} and Ψ_{50}. The 1:1 line (continuous line) and the quantile 99% (dashed line) are shown. The orange line is the best fit with a segmented regression, showing a significant breakpoint for Ψ_{50} of −5.9 MPa or Ψ_{12} of −4.2 MPa corresponding to an average Ψ_{close} of about −3 MPa (± 1.5 MPa, 95% CI). The inset in (c) shows the linear relationship between the safety margins between stomatal closure and embolism formation (Ψ_{close}- Ψ_{12}) and Ψ_{12} ($P < 0.01$). In (c) and (d), the points correspond to individual species, with pictograms highlighting the different functional and taxonomic groups, as indicated in the legend to (d).

water deficit), precluding direct comparisons of survival between the four studies considered. We therefore used (1) a generalised mixed-effects model showing a significant effect of ψ_{50} on T_{50} ($P = 0.0003$) and a significant interaction between ψ_{50} and experiment (study) ($P = 0.0128$) (Appendix S1), and (2) a standardised T_{50} for each experiment taking into account the differences in soil volume (Appendix S1).

RESULTS AND DISCUSSION

Embolism resistance (taken as Ψ_{50}) ranged between −1.3 and −19 MPa (Fig. 1a). The large variations of Ψ_{50} were partly related to changes in *slope,* which was non-linearly related to Ψ_{50} (Fig. 1a, insert). Ψ_{50} and *slope* together determined the water potential causing the onset of embolism (Ψ_{12}). This more conservative indicator of embolism resistance ranged between −0.7 and −14 MPa. The two indicators of water potential causing stomatal closure (Ψ_{close}) were significantly related to each other, with a slope close to one ($P < 0.01$ Fig. 1b, inset), as previously reported (Mencuccini *et al.* 2015; Bartlett *et al.* 2016), Ψ_{close} was thus taken as the average value when the two traits were available. Ψ_{close} varied from −1. to −4.3 MPa, spanning a range of variation only one-third that for embolism resistance (Fig. 1a and b), consistent with the findings of recent meta-analysis (Mencuccini *et al.* 2015; Bartlett *et al.* 2016).

Our meta-analysis showed that most species have Ψ_{close} values that are higher than their Ψ_{50} or Ψ_{12} values (Fig. 1c and d). The difference between Ψ_{50} and Ψ_{close}, defined as the safety margin between stomatal closure and embolism formation (SM_{P50}) was greater than zero for 99% of the species studied, and SM_{P12} was greater than zero for 67% of the species studied (Fig. S2). This finding is not consistent with the expected coordination between stomatal closure and embolism resistance based on small safety margins to ensure the maintenance of CO_2 assimilation for as long as possible during drought (Tyree & Sperry 1988). The 1:1 line (in Fig. 1c and d) therefore appears to define a first boundary to plant hydraulics. We also found that safety margins increased continuously with increasing embolism resistance (Fig. 1c insert). This relationship reflects the low slope value of 0.4 for species with low embolism resistance and the segmented relationship between Ψ_{close} and embolism resistance for high embolism resistance (Fig. 1c and 1d, summary statistics and

comparisons with other models are provided in Table S2). Break-points for the segmented relationships were found for $\Psi_{12} = -4.5$ and $\Psi_{50} = -6$ MPa, corresponding to a $\Psi_{close} = -3$ MPa on average (Fig. 1c and d and Table S3). Ψ_{close} reached a plateau at −4 MPa (1st percentile of the distribution), even for species highly resistant to embolism. A second boundary is thus defined by the limit of Ψ_{close}. Overall, these patterns were also observed within the different taxonomic (gymnosperm and angiosperm) and functional (evergreen and deciduous) groups tested and they were not affected by consideration of the two indicators for Ψ_{close} separately (Fig. 1c and d, Figure S3, Figure S4, Table S3).

The vascular system of terrestrial plants has evolved towards very high levels of embolism resistance (Delzon *et al.* 2010; Pittermann *et al.* 2012; Larter *et al.* 2017), reaching Ψ_{50} values down to −19 MPa, which is close to the practical limit of water metastability, suggesting that liquid water transport under the cohesion-tension theory has reached its operational boundary in these aridity-resistant species (Larter *et al.* 2015). It could be hypothesised that stomatal closure has evolved along similar lines, to maintain gas exchange (e.g. for carbon assimilation and transpiration) for longer periods during drought, even at low xylem water potential. However, our findings conflict with this view, suggesting that stomatal closure is subject to additional constraints. A physiological limit to stomata opening at low water potential may arise due to the deleterious effects of the solute accumulation in leaves (i.e. osmotic adjustment) required to maintain turgor pressure and stomatal opening. Excessive solute accumulation may lead to precipitation, severely impairing protein activity. However, van't Hoff's law predicts solute precipitation at osmotic potentials far below (<−10 MPa for KCl or sugars) the values of Ψ_{close} reported in our database. This uncoupling of stomatal closure and embolism resistance may alternatively result from selection pressures that have favoured survival under extreme water scarcity over growth under mild drought conditions. This greater safety margin between stomatal closure and embolism formation would have allowed plants to adapt to extreme drought conditions and to colonise xeric environments.

We investigated this pattern further, using the SurEau model to calculate survival times under drought conditions (i.e. the time to reach 100% loss of hydraulic conductance) for a range of hypothetical species covering the full spectrum encountered in our database. Three hypotheses for the stomatal regulation of E were used to evaluate how the interplay between stomatal closure and embolism resistance shapes survival under drought conditions (Fig. 2a, see Methods and Appendix S2). Under the hypothesis of no stomatal closure during drought (i.e. Hypothesis 1, Fig. 2a), plants would die very rapidly from hydraulic failure, with only a slight increase in survival when Ψ_{50} decreased from −1 to −6 MPa (Fig. 2c). For Ψ_{50} values below −6 MPa, increasing embolism resistance was not associated with a further increase in survival time. Despite their simplicity, these control simulations indicate that increasing embolism resistance *per se* has only a marginal impact on survival under drought conditions, particularly for highly resistant species.

Under the assumption that stomata should close at the onset of embolism (i.e. Hypothesis 2, where $\Psi_{close} = \Psi_{12}$, Fig. 2b), a much higher mean survival time was obtained (Fig. 2b). Survival also increased markedly with embolism resistance until a Ψ_{50} of −6 MPa. However, beyond this value, survival decreased substantially (Fig. 2b), contrary to the trend observed in analyses of experimentally induced mortality (Fig. 2c). This increase in survival at high Ψ_{50} (Ψ_{50}>−6 MPa) values is due to the maintenance of Ψ_{12} (and thus of stomatal closure) at an almost constant value of about −3 MPa, due to the decrease in the *slope* of the VC with decreasing Ψ_{50} (Appendix SA2–4, Fig. A2–6). Under this assumption, if the *slope* of the VC was maintained at a constant mean value for all the values of Ψ_{50} tested, the model would simulate a continuous decrease in survival for all levels of Ψ_{50} tested (Appendix S2–2, Fig. A2–2). The survival peak simulated at a Ψ_{50} of −6 MPa (Fig. 2b) under this hypothesis implied a Ψ_{close} value of about −3 MPa, corresponding to the mean limit for Ψ_{close} in our database. Thus, assuming that Ψ_{close} does not covary with embolism resistance beyond $\Psi_{close} = -3$ MPa (hypothesis 3, Fig. 2a), a positive relationship between survival and embolism resistance was predicted over the entire range of Ψ_{50} (Fig. 2b), consistent with the empirical trend observed in drought mortality experiments (Fig. 2c). These simulations support the view that embolism resistance cannot increase survival unless the difference between embolism resistance and Ψ_{close} also increases.

An analysis of the modelled dynamics of soil and plant dehydration for two species with contrasting levels of embolism resistance identified the physical mechanisms making early stomata closure necessary for the avoidance of drought-induced mortality, even for embolism-resistant species (Fig. 3). The relationship between soil water potential (Ψ_{soil}) (and, hence, plant water potential) and soil water content (θ) becomes nonlinear at relatively high values of Ψ_{soil} (Fig. 3a and b). Thus, the longer transpiration is maintained, the sharper the rates of decrease in soil and plant water potential, leading to rapid death through hydraulic failure. The nonlinearity of the Ψ_{soil} (θ) relationship results from long-established physical laws (Campbell 1974; van Genuchten 1980) describing the changes in Ψ_{soil} and soil conductivity with soil water content. These laws are globally conserved among soil types (Appendix A4, Figure A4–1), providing support for the overall scope of our findings.

The vascular system of terrestrial plants has evolved towards very high levels of embolism resistance (Ψ_{50} values down to −19 MPa), enabling plants to colonise dry environments (Pittermann *et al.* 2012; Larter *et al.* 2017). Stomatal closure might have been expected to have evolved along similar lines, to maintain carbon assimilation levels for longer periods, even at low xylem water potential. Moreover, several recent studies have reported close covariation between stomatal closure in response to drought and embolism resistance, but only for species with relatively low levels of drought resistance (Cruiziat *et al.* 2002; Klein 2014; Mencuccini *et al.* 2015; Bartlett *et al.* 2016). Our results indicate that the range of variation of Ψ_{close} is much smaller when considered in the light of the full range of embolism resistance. This uncoupling of stomatal closure and vascular system failure may result

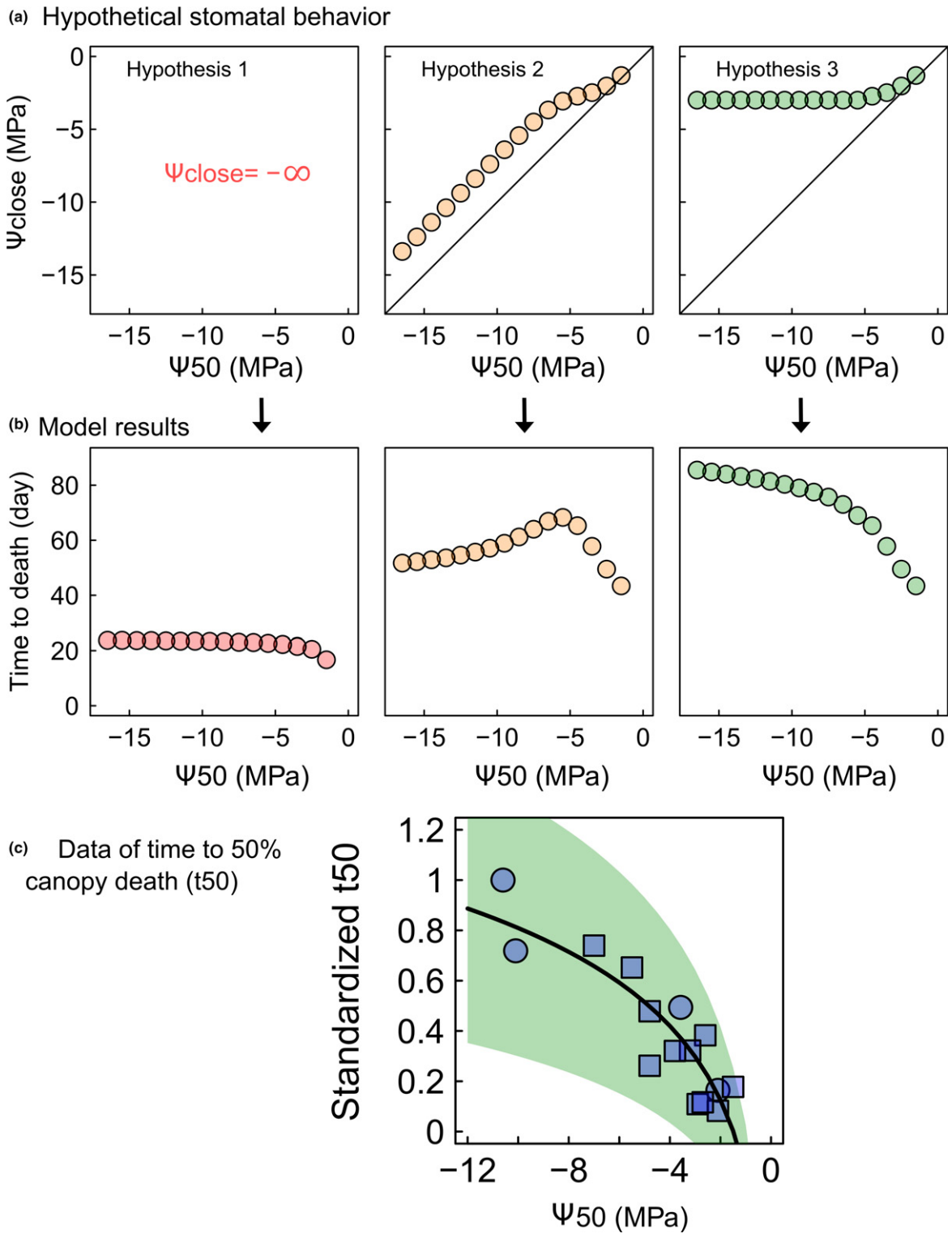

Figure 2 Model simulations of survival time for the full range of embolism resistance, under three different hypotheses concerning stomatal behaviour. (a) Representation of the parameter combinations for Ψ_{close} and Ψ_{50} used to represent the three hypotheses tested in the model: (Hypothesis 1) Stomata never close (i.e. plants maintain maximal rates of transpiration at all soil and plant water potentials, whatever their Ψ_{50}). Hypothesis 1 is used as a control, to assess the effect of stomatal closure under the other hypotheses. (Hypothesis 2) Stomata gradually close with turgor loss, such that water potential at full closure (Ψ_{close}) equals Ψ_{12} (i.e. tight coordination between Ψ_{close} and Ψ_{12}). (Hypothesis 3) Stomatal closure and embolism resistance are equal only to −3 MPa, as indicated by our empirical results (Fig. 1). (b) Simulated relationship between survival time (time to reach 100% of PLC) and Ψ_{50} for each hypothesis tested. With the exception of the changes to E regulation made to satisfy the hypothesis tested, all other parameters were kept constant (Appendix S4). (c) Normalised time to 50% shoot death (T_{50}) as a function of Ψ_{50} for 15 species. The data were collected from four different studies and normalised to account for differences in soil and climate conditions across experiments (see Methods). The logarithmic relationship fitted to absolute values ($0.42 \times \log(|\psi_{50}|) - 0.16$, slope $P < 0.001$) is shown (line) with its 95% CI (green area).

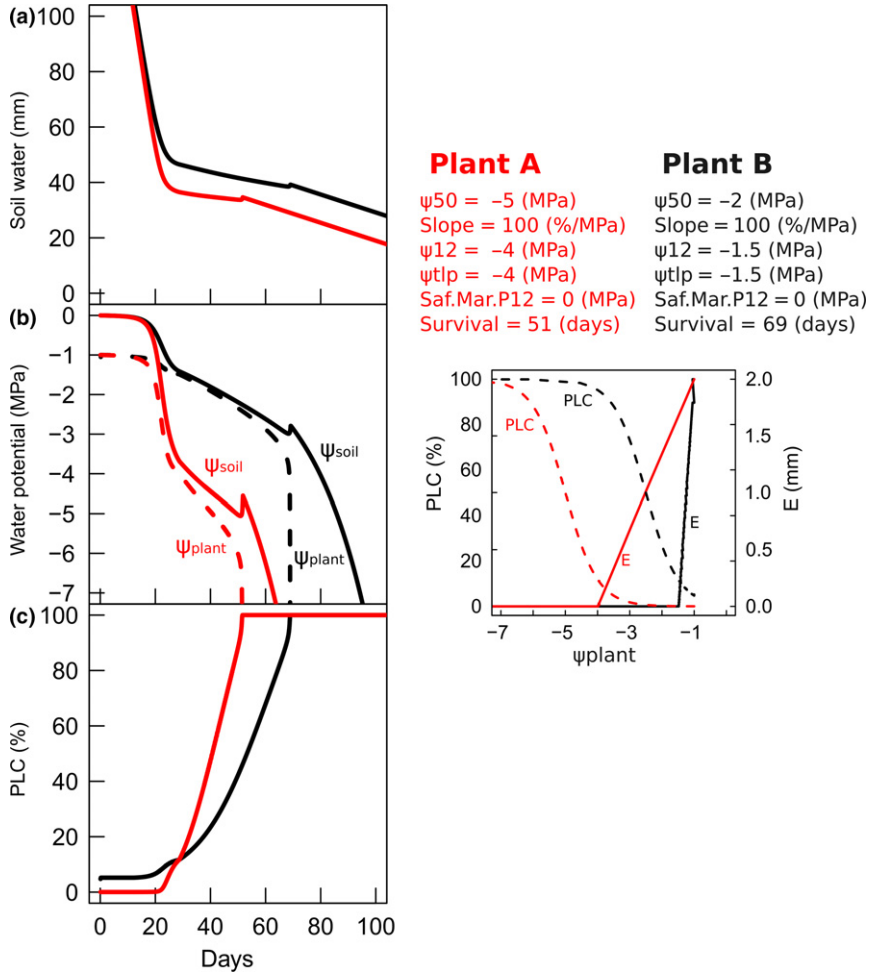

Figure 3 Simulated temporal dynamics of soil and plant dehydration assuming that stomata gradually close to reach full closure at $\Psi = \Psi_{12}$ (hypothesis 2) for two species with different stomata and hydraulic traits, as described in the right panel. (a) Soil water content, (b) soil and plant water potential and (c) the percent loss of conductivity caused by embolism. Simulations were performed for two hypothetical plants (plant a and plant b), the traits of which are shown in MPa on the plot. The time to death from hydraulic failure (i.e. 100% embolism) is also indicated above the right panel. Simulations show that higher levels of embolism resistance and, thus, higher water potential at full stomatal closure accelerate death, due to a faster decrease in water potential. More detailed simulation results are provided in Appendix S2.

from selection pressures that have favoured survival under conditions of extreme water scarcity over growth under mild drought conditions.

These findings provide a view complementary to the widely accepted framework for drought response strategies based on the water-to-carbon trade-off [e.g.(McDowell *et al.* 2008; Skelton *et al.* 2015; Yoshimura *et al.* 2016)]. According to this framework, plant drought response strategies lie between two extreme categories: isohydric and anisohydric (McDowell *et al.* 2008; Klein 2014; Martinez-Vilalta *et al.* 2014). Isohydric plants close their stomata rapidly in response to drought, thereby maintaining a high water potential to limit embolism, but at the risk of death due to carbon starvation. Conversely, anisohydric plants keep their stomata open at low water potential, maintaining carbon assimilation levels, but at the cost of damage to the water transport system due to embolism. This framework has been the focus of many scientific studies on drought-induced mortality in recent decades and underpins the current understanding and modelling of drought-induced plant mortality (McDowell *et al.* 2008; Skelton *et al.* 2015; Yoshimura *et al.* 2016). The finding that the most drought-resistant plants close their stomata at a potential much higher than that at which embolism can occur indicates that drought resistance may not involve the maintenance of gaseous exchanges during drought conditions. Indeed, it demonstrates that, on the contrary, plants have to limit decreases in water potential, as confirmed by the modelling analysis (Fig. 2b).

The relatively low variation of Ψ_{close} relative to Ψ_{50} may appear to conflict with the large variations in minimum water potential reported by various studies (Choat *et al.* 2012; Martinez-Vilalta *et al.* 2014; Anderegg *et al.* 2016; Martínez-Vilalta & Garcia-Forner 2016). However, it may highlight the importance of accounting for the multiple traits driving the demand for water when stomata are closed in representations of water potential decline and, thus, plant dehydration. For instance, the minimum leaf conductance (i.e. when stomata are closed) and leaf area are important traits driving plant water potential decline. The hydraulic model presented here is consistent with this view. Accordingly, model simulations indicated that there were two main stages defining the temporal

sequence leading to plant desiccation in situations of water scarcity (Fig. 3). The first of these stages is defined by the time between the start of water shortage and stomatal closure. Its duration depends principally on the rate of water uptake, given the relative constancy of Ψ_{close} in plants and the competition between plants for water in community ecosystems. The second stage is defined by the time between stomatal closure and plant death (100% embolism). The duration of this stage depends on a set of drought resistance traits allowing plant tissues to retain water under very high tension, to decrease water loss when the stomata are closed and to limit the decrease in water potential during embolism through deeper rooting or the release of water from internal stores (Blackman *et al*. 2016). It remains to be seen how these other traits covary with embolism resistance, are coordinated and have coevolved to shape the spectrum of drought adaptation strategies in plants. However, the conclusions drawn here at the plant scale may require adjustment at a later stage, when improvements in experimental methodology allow reliable measurements of leaf and fine root xylem vulnerability to be incorporated into the model.

Overall, the model analysis presented here demonstrates that multiple measurable drought resistance traits can be integrated into a consistent and thermodynamically reliable formal framework to define drought-induced mortality (Pivovaroff *et al*. 2016). This modelling approach must be validated carefully against the temporal dynamics of water potential, hydraulic conductance, data for embolism proper, and experimental and field mortality for different species. The model will need to evolve with advances in our understanding of plant hydraulics, to explore mechanisms that are expected to be important for plant survival, such as hydraulic segmentation, the role of plant capacitance or the impact of cuticular transpiration on energy balance, critical leaf temperatures and plant desiccation. However, in its present form, it constitutes an important step in assessments of the consequences of drought in land plants and the effects of climate change on terrestrial ecosystem functions. It may also prove to be a powerful tool for taking multiple traits into account in breeding strategies.

ACKNOWLEDGMENTS

Over the last 10 years, the research on these topics conducted at INRA has received funding from INRA-EFPA division, the 'Investments for the Future' program (grant no. ANR-10-EQPX-16, XYLOFOREST) from the French National Agency for Research, the Cluster of Excellence COTE (ANR-10-LABX-45, Water Stress and Vivaldi projects), and the PitBulles project (ANR no. 2010 Blanc 171001) and for the ERC project TREEPEACE (FP7-339728). We thank Regis Burlett and Gaëlle Capdeville (UMR BIOGECO), Pierre Conchon and Romain Souchal (UMR PIAF) and the Experimental Unit of Pierroton for their assistance with xylem embolism vulnerability measurements.

AUTHORS' CONTRIBUTIONS

NM, SD and HC conceived the idea for this work. NM assembled the data set and analysed the data with inputs from SD. HC developed a preliminary version of the SurEau model. NM implemented the model under R and performed the computational analysis. NM wrote the manuscript with revisions from SD and HC.

DATA ACCESSIBILITY

The Database is fully available in zenodo repository: DOI: 10.5281/zenodo.854700 (https://zenodo.org/record/854700#.WabculpyuU)

REFERENCES

Allen, C.D., Macalady, A.K., Chenchouni, H., Bachelet, D., McDowell, N., Vennetier, M. *et al*. (2010). A global overview of drought and heat-induced tree mortality reveals emerging climate change risks for forests RID B-9318-2009. *For. Ecol. Manage*., 259, 660–684.

Anderegg, W.R.L., Kane, J.M. & Anderegg, L.D.L. (2012). Consequences of widespread tree mortality triggered by drought and temperature stress. *Nat. Clim. Chang*., 3, 30–36.

Anderegg, W.R.L., Klein, T., Bartlett, M., Sack, L., Pellegrini, A.F.A., Choat, B. *et al*. (2016). Meta-analysis reveals that hydraulic traits explain cross-species patterns of drought-induced tree mortality across the globe. *Proc. Natl Acad. Sci. USA*, 113, 5024–5029.

Barigah, T.S., Charrier, O., Douris, M., Bonhomme, M., Herbette, S., Améglio, T. *et al*. (2013). Water stress-induced xylem hydraulic failure is a causal factor of tree mortality in beech and poplar. *Ann. Bot*., 112, 1431–1437.

Bartlett, M.K., Klein, T., Jansen, S., Choat, B. & Sack, L. (2016). The correlations and sequence of plant stomatal, hydraulic, and wilting responses to drought. *Proc. Natl Acad. Sci. USA*, 113, 13098–13103.

Beikircher, B., Ameglio, T., Cochard, H. & Mayr, S. (2010). Limitation of the Cavitron technique by conifer pit aspiration. *J. Exp. Bot*., 61, 3385–3393.

Bessey, C.E. (1898). Some considerations upon the functions of stomata. *Science*, 7, 13–16.

Blackman, C.J., Pfautsch, S., Choat, B., Delzon, S., Gleason, S.M. & Duursma, R.A. (2016). Toward an index of desiccation time to tree mortality under drought. *Plant, Cell Environ*., 39, 2342–2345.

Bouche, P.S., Jansen, S., Cochard, H., Burlett, R., Capdeville, G. & Delzon, S. (2015). Embolism resistance of conifer roots can be accurately measured with the flow-centrifuge method. *J. Plant Hydraul*., 2, e002.

Bouche, P.S., Delzon, S., Choat, B., Badel, E., Brodribb, T.J., Burlett, R. *et al*. (2016a). Are needles of *Pinus pinaster* more vulnerable to xylem embolism than branches? New insights from X-ray computed tomography. *Plant, Cell Environ*., 39, 860–870.

Bouche, P.S., Jansen, S., Sabalera, J.C., Cochard, H., Burlett, R. & Delzon, S. (2016b). Low intra-tree variability in resistance to embolism in four Pinaceae species. *Ann. For. Sci*., 73, 681–689.

Brodribb, T.J. & Cochard, H. (2009). Hydraulic failure defines the recovery and point of death in water-stressed conifers. *Plant Physiol*., 149, 575–584.

Brodribb, T.J., Holbrook, N.M., Edwards, E.J., Gutiérrez, M.V. & Gutierrez, M.V. (2003). Relations between stomatal closure, leaf turgor and xylem vulnerability in eight tropical dry forest trees. *Plant, Cell Environ*., 26, 443–450.

Brodribb, T.J., McAdam, S.A.M.M., Jordan, G.J. & Martins, S.C.V.V. (2014). Conifer species adapt to low-rainfall climates by following one of two divergent pathways. *Proc. Natl Acad. Sci. USA*, 111, 1–5.

Buckley, T.N. (2005). The control of stomata by water balance. *New Phytol*., 168, 275–291.

Campbell, G.S. (1974). A simple method for determining unsaturated conductivity from moisture retention data. *Soil Sci*., 117, 311–314.

Carnicer, J., Coll, M., Ninyerola, M., Pons, X., Sanchez, G. & Penuelas, J. (2011). Widespread crown condition decline, food web disruption,

and amplified tree mortality with increased climate change-type drought. *Proc. Natl Acad. Sci. USA*, 108, 1474–1478.
Choat, B., Jansen, S., Brodribb, T.J., Cochard, H., Delzon, S., Bhaskar, R. *et al.* (2012). Global convergence in the vulnerability of forests to drought. *Nature*, 491, 752–755.
Choat, B., Brodersen, C.R. & McElrone, A.J. (2014). Synchrotron X-ray microtomography of xylem embolism in *Sequoia sempervirens* saplings during cycles of drought and recovery. *New Phytol.*, 205, 1095–1105.
Choat, B., Badel, E., Burlett, R., Delzon, S., Cochard, H. & Jansen, S. (2016). Noninvasive measurement of vulnerability to drought-induced embolism by X-ray microtomography. *Plant Physiol.*, 170, 273–282.
Ciais, P., Reichstein, M., Viovy, N., Granier, A., Ogee, J., Allard, V. *et al.* (2005). Europe-wide reduction in primary productivity caused by the heat and drought in 2003. *Nature*, 437, 529–533.
Cochard, H., Badel, E., Herbette, S., Delzon, S., Choat, B. & Jansen, S. (2013). Methods for measuring plant vulnerability to cavitation: a critical review. *J. Exp. Bot.*, 64, 4779–4791.
Cochard, H., Delzon, S. & Badel, E. (2015). X-ray microtomography (micro-CT): a reference technology for high-resolution quantification of xylem embolism in trees. *Plant, Cell Environ.*, 38, 201–206.
Cowan, I.R. (1965). Transport of water in the soil-plant-atmosphere continuum. *J. Appl. Ecol.*, 2, 221–239.
Cruiziat, P., Cochard, H. & Améglio, T. (2002). Hydraulic architecture of trees: main concepts and results. *Ann. For. Sci.*, 59, 723–752.
Cuneo, I.F., Knipfer, T., Brodersen, C.R. & McElrone, A.J. (2016). Mechanical failure of fine root cortical cells initiates plant hydraulic decline during drought. *Plant Physiol.*, 172, 1669–1678.
Darwin, F. (1898). Observations on stomata. *Philos. Trans. R. Soc. B Biol. Sci.*, 190, 531–621.
Delzon, S., Douthe, C., Sala, A. & Cochard, H. (2010). Mechanism of water stress-induced cavitation in conifers: bordered pit structure and function support the hypothesis of seal capillary seeding. *Plant, Cell Environ.*, 33, 2101–2111.
Flexas, J. & Medrano, H. (2002). Drought-inhibition of photosynthesis in C-3 plants: stomatal and non-stomatal limitations revisited. *Ann. Bot.*, 89, 183–189.
Franks, P.J., Cowan, I.R. & Farquhar, G.D. (1998). A study of stomatal mechanics using the cell pressure probe. *Plant, Cell Environ.*, 21, 94–100.
Gardner, W.R. (1964). Relation of root distribution to water uptake and availability. *Agron. J.*, 56, 41–55.
van Genuchten, M.T. (1980). A closed-form equation for predicting the hydraulic conductivity of unsaturated soils. *Soil Sci. Soc. Am. J.*, 44, 892–898.
Hölttä, T., Cochard, H., Nikinmaa, E. & Mencuccini, M. (2009). Capacitive effect of cavitation in xylem conduits: results from a dynamic model. *Plant, Cell Environ.*, 32, 10–21.
Jones, H.G. & Sutherland, R.A. (1991). Stomatal control of xylem embolism. *Plant, Cell Environ.*, 14, 607–612.
Klein, T. (2014). The variability of stomatal sensitivity to leaf water potential across tree species indicates a continuum between isohydric and anisohydric behaviours. *Funct. Ecol.*, 28, 1313–1320.
Larter, M., Brodribb, T.J., Pfautsch, S., Burlett, R., Cochard, H. & Delzon, S. (2015). Extreme aridity pushes trees to their physical limits. *Plant Physiol.*, 168, 804–807.
Larter, M., Pfautsch, S., Domec, J.C., Trueba, S., Nagalingum, N. & Delzon, S. (2017). Aridity drove the evolution of extreme embolism resistance and the radiation of conifer genus *Callitris*. *New Phytol.*, 215, 97–112.
Lens, F., Picon-Cochard, C., EL Delmas, C., Signarbieux, C., Buttler, A., Cochard, H. *et al.* (2016). Herbaceous angiosperms are not more vulnerable to drought-induced embolism than angiosperm trees. *Plant Physiol.*, 172, 661–667.
Li, S., Feifel, M., Karimi, Z., Schuldt, B., Choat, B. & Jansen, S. (2015). Leaf gas exchange performance and the lethal water potential of five European species during drought. *Tree Physiol.*, 36, 179–192.
Maherali, H.A., Pockman, W.T., Wi, T.P. & Jackson, R.B. (2004). Adaptive variation in the vulnerability of woody plants to xylem cavitation. *Ecology*, 85, 2184–2199.
Martínez-Vilalta, J. & Garcia-Forner, N. (2016). Water potential regulation, stomatal behaviour and hydraulic transport under drought: deconstructing the iso/anisohydric concept. *Plant, Cell Environ.*, 40, 962–976.
Martinez-Vilalta, J., Poyatos, R., Aguad, D., Retana, J. & Mencuccini, M. (2014). A new look at water transport regulation in plants. *New Phytol.*, 204, 105–115.
McDowell, N., Pockman, W.T., Allen, C.D., Breshears, D.D., Cobb, N., Kolb, T. *et al.* (2008). Mechanisms of plant survival and mortality during drought: why do some plants survive while others succumb to drought? *New Phytol.*, 178, 719–739.
McDowell, N.G., Fisher, R.A., Xu, C., Domec, J.C., Hölttä, T., Mackay, D.S. *et al.* (2013). Evaluating theories of drought-induced vegetation mortality using a multimodel-experiment framework. *New Phytol.*, 200, 304–321.
Mencuccini, M., Minunno, F., Salmon, Y. & Mart, J. (2015). Coordination of physiological traits involved in drought-induced mortality of woody plants. *New Phytol.*, 208, 396–409.
Mualem, Y. (1976). A new model for predicting the hydraulic conductivity of unsaturated porous media. *Water Resour. Res.*, 12, 57–64.
Park Williams, A., Alle 1. Park Williams, A. et al. (2012) Temperature as a potent driver of regional forest drought stress and tree mortality. *Nat. Clim. Chang.* 3, 292–297.
Pittermann, J., Stuart, S. A, Dawson, T.E. & Moreau, A. (2012). Cenozoic climate change shaped the evolutionary ecophysiology of the Cupressaceae conifers. *Proc. Natl Acad. Sci. USA*, 109, 9647–9652.
Pivovaroff, A.L., Pasquini, S.C., De Guzman, M.E., Alstad, K.P., Stemke, J.S. & Santiago, L.S. (2016). Multiple strategies for drought survival among woody plant species. *Funct. Ecol.*, 30, 517–526.
Rambal, S. (1993). The differential role of mechanisms for drought resistance in a Mediterranean evergreen shrub: a simulation approach. *Plant, Cell Environ.*, 16, 35–44.
Rodriguez-Dominguez, C.M., Buckley, T.N., Egea, G., de Cires, A., Hernandez-Santana, V., Martorell, S. *et al.* (2016). Most stomatal closure in woody species under moderate drought can be explained by stomatal responses to leaf turgor. *Plant, Cell Environ.*, 39, 2014–2026.
Scoffoni, C., Albuquerque, C., Brodersen, C., Townes, S.V., John, G.P., Bartlett, M.K. *et al.* (2017). Outside-xylem vulnerability, not xylem embolism, controls leaf hydraulic decline during dehydration. *Plant Physiol.*, 173, 1197–1210.
Skelton, R.P., West, A.G. & Dawson, T.E. (2015). Predicting plant vulnerability to drought in biodiverse regions using functional traits. *Proc. Natl Acad. Sci. USA*, 112, 5744–5749.
Skelton, R.P., Brodribb, T.J. & Choat, B. (2017). Casting light on xylem vulnerability in an herbaceous species reveals a lack of segmentation. *New Phytol.*, 214, 561–569.
Sperry, J.S. (2004). Coordinating stomatal and xylem functioning - an evolutionary perspective. *New Phytol.*, 162, 568–570.
Sperry, J.S., Adler, F.R., Campbell, G.S. & Comstock, J.P. (1998). Limitation of plant water use by rhizosphere and xylem conductance: results from a model. *Plant, Cell Environ.*, 21, 347–359.
Tardieu, F., Bruckler, L. & Lafolie, F. (1992). Root clumping may affect the root water potential and the resistance to soil-root water transport. *Plant Soil*, 140, 291–301.
Torres-Ruiz, J.M., Jansen, S., Choat, B., McElrone, A.J., Cochard, H., Brodribb, T.J. *et al.* (2015). Direct X-ray microtomography observation confirms the induction of embolism upon xylem cutting under tension. *Plant Physiol.*, 167, 40–43.
Tuzet, A., Perrier, A. & Leuning, R. (2003). A coupled model of stomatal conductance, photosynthesis and transpiration. *Plant, Cell Environ.*, 26, 1097–1116.
Tyree, M.T. & Ewers, F.W. (1991). The hydraulic architecture of trees and other woody plants. *New Phytol.*, 119, 345–360.
Tyree, M.T. & Sperry, J.S. (1988). Do woody plants operate near the point of catastrophic xylem dysfunction caused by dynamic water stress?: answers from a model. *Plant Physiol.*, 88, 574–580.

Tyree, M.T. & Yang, S. (1990). Water-storage capacity of *Thuja, Tsuga* and *Acer* stems measured by dehydration isotherms - The contribution of capillary water and cavitation. *Planta*, 182, 420–426.

Urli, M., Porte, A.J., Cochard, H., Guengant, Y., Burlett, R. & Delzon, S. (2013). Xylem embolism threshold for catastrophic hydraulic failure in angiosperm trees. *Tree Physiol*., 33, 672–683.

Vander Willigen, C. & Pammenter, N.W. (1998). Relationship between growth and xylem hydraulic characteristics of clones of *Eucalyptus* spp. at contrasting sites. *Tree Physiol*., 18, 595–600.

Vitali, M., Cochard, H., Gambino, G., Ponomarenko, A., Perrone, I. & Lovisolo, C. (2016). VvPIP2;4N aquaporin involvement in controlling leaf hydraulic capacitance and resistance in grapevine. *Physiol. Plant*., 158, 284–296.

Whitehead, D. & Jarvis, P.G. (1981). Water deficits and plant growth. In: *Coniferous Forests and Plantations* (ed Kozlowski, T.). Academic Press, VI, New York, NY, pp. 49–152.

Yoshimura, K., Saiki, S.-T., Yazaki, K., Ogasa, M.Y., Shirai, M., Nakano, T. *et al.* (2016). The dynamics of carbon stored in xylem sapwood to drought-induced hydraulic stress in mature trees. *Sci. Rep*., 6, 24513.

SUPPORTING INFORMATION

Additional Supporting Information may be found online in the supporting information tab for this article.

Editor, Hafiz Maherali
Manuscript received 1 June 2017
First decision made 4 July 2017
Manuscript accepted 17 August 2017